



1 **N₂O₅ uptake onto saline mineral dust: a potential missing source of tropospheric**
2 **ClNO₂ in inland China**

3

4 Haichao Wang^{1,#}, Chao Peng^{2,#}, Xuan Wang^{3,#}, Shengrong Lou⁴, Keding Lu⁵, Guicheng Gan⁶,
5 Xiaohong Jia¹, Xiaorui Chen⁵, Jun Chen⁶, Hongli Wang⁴, Shaojia Fan^{1,7}, Xinming Wang^{2,8,9}
6 Mingjin Tang^{2,8,9,*}

7

8 ¹ School of Atmospheric Sciences, Sun Yat-sen University, Guangzhou, China

9 ² State Key Laboratory of Organic Geochemistry, Guangdong Key Laboratory of Environmental
10 Protection and Resources Utilization, and Guangdong-Hong Kong-Macao Joint Laboratory for
11 Environmental Pollution and Control, Guangzhou Institute of Geochemistry, Chinese Academy of
12 Sciences, Guangzhou, China

13 ³ School of Energy and Environment, City University of Hong Kong, Hong Kong SAR, China

14 ⁴ State Environmental Protection Key Laboratory of Formation and Prevention of the Urban Air
15 Complex, Shanghai Academy of Environmental Sciences, Shanghai, China

16 ⁵ State Key Joint Laboratory of Environmental Simulation and Pollution Control, College of
17 Environmental Sciences and Engineering, Peking University, Beijing, China

18 ⁶ Institute of Particle and Two-Phase Flow Measurement, College of Energy and Power
19 Engineering, University of Shanghai for Science and Technology, Shanghai, China

20 ⁷ Guangdong Provincial Observation and Research Station for Climate Environment and Air
21 Quality Change in the Pearl River Estuary, Key Laboratory of Tropical Atmosphere-Ocean System,
22 Ministry of Education, Southern Marine Science and Engineering Guangdong Laboratory
23 (Zhuhai), Zhuhai, China



24 ⁸ CAS Center for Excellence in Deep Earth Science, Guangzhou 510640, China

25 ⁹ University of Chinese Academy of Sciences, Beijing, China

26

27 #These authors contributed equally to this work

28 *correspondence: Mingjin Tang (mingjintang@gig.ac.cn)

29



30 **Abstract**

31 Nitryl chloride (ClNO₂), an important precursor of Cl atoms, significantly affects atmospheric
32 oxidation capacity and O₃ formation. However, sources of ClNO₂ in inland China have not been
33 fully elucidated. In this work, laboratory experiments were conducted to investigate heterogeneous
34 reaction of N₂O₅ with eight saline mineral dust samples collected from different regions in China,
35 and substantial formation of ClNO₂ was observed. ClNO₂ yields, $\phi(\text{ClNO}_2)$, showed large
36 variations (ranging from <0.05 to ~0.77) for different saline mineral dust samples, largely
37 depending on mass fractions of particulate chloride. In addition, for different saline mineral dust
38 samples, $\phi(\text{ClNO}_2)$ could increase, decrease or show insignificant change as RH increased from
39 18% to 75%. We further found that current parameterizations significantly overestimated $\phi(\text{ClNO}_2)$
40 for heterogeneous uptake of N₂O₅ onto saline mineral dust. Assuming a uniform $\phi(\text{ClNO}_2)$ value
41 of 0.10 for N₂O₅ uptake onto mineral dust, we used a 3-D chemical transport model to assess the
42 impact of this reaction on tropospheric ClNO₂ in China, and found that weekly mean nighttime
43 maximum ClNO₂ mixing ratios could be increased by up to 85 pptv during a severe dust event in
44 May 2017. Overall, our work showed that heterogeneous reaction of N₂O₅ with saline mineral dust
45 could be an important source of tropospheric ClNO₂ in inland China.

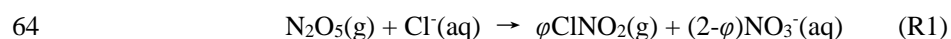
46



47 **1 Introduction**

48 The formation of O₃ and secondary aerosols, two major air pollutants, is closely related to
49 atmospheric oxidation processes (Lu et al., 2019). Primary pollutants emitted by natural and
50 anthropogenic sources are oxidized by various oxidants to produce O₃ and secondary aerosols,
51 affecting air quality and climate. Major tropospheric oxidants include OH radicals, NO₃ radicals
52 and O₃, and in the last two decades Cl atoms have been proposed as an important oxidant (Saiz-
53 Lopez and von Glasow, 2012; Simpson et al., 2015; Wang et al., 2019). Rate constants for reactions
54 of certain volatile organic compounds (VOCs) with Cl atoms can be a few orders of magnitude
55 larger than those reacting with OH radicals (Atkinson and Arey, 2003; Atkinson et al., 2006);
56 therefore, despite its lower concentrations in the troposphere, Cl can contribute significantly to
57 atmospheric oxidation capacity in some regions (Saiz-Lopez and von Glasow, 2012; Simpson et
58 al., 2015; Wang et al., 2019). For example, a modeling study (Sarwar et al., 2014) suggested that
59 including Cl chemistry in the model could enhance oxidative degradation of VOCs by >20% in
60 some locations.

61 One major source of tropospheric Cl atoms is daytime photolysis of ClNO₂ (Thornton et al.,
62 2010; Simpson et al., 2015), which is formed in heterogeneous reaction of N₂O₅ with chlorine-
63 containing particles (R1) at nighttime (Osthoff et al., 2008; Thornton et al., 2010):



65 The uptake coefficient, $\gamma(\text{N}_2\text{O}_5)$, and the ClNO₂ yield, $\varphi(\text{ClNO}_2)$, both depend on relative humidity
66 (RH), aerosol composition and mixing state, and etc. (Bertram and Thornton, 2009; Ryder et al.,
67 2014; Mitroo et al., 2019; McNamara et al., 2020; Yu et al., 2020). Cl atoms produced by ClNO₂
68 photolysis can effectively enhance atmospheric oxidation (Le Breton et al., 2018; Wang et al.,
69 2019) and thus increase concentrations of O₃ and OH radicals during the day (Simon et al., 2009;



70 Riedel et al., 2014; Sarwar et al., 2014; Tham et al., 2016; Wang et al., 2016). In addition, ClNO₂
71 is an important temporary reservoir of NO_x at night and releases NO₂ during the daytime via
72 photolysis, thereby further affecting daytime photochemistry.

73 Sea spray aerosol is the most important source of particulate chloride (Cl⁻), and ClNO₂ is
74 expected to be abundant at marine and coastal regions impacted by anthropogenic emissions. High
75 levels of ClNO₂ have been observed at various marine and coastal regions over the globe (Simon
76 et al., 2009; Riedel et al., 2012; Tham et al., 2014; Young et al., 2014; Wang et al., 2016; Osthoff
77 et al., 2018; Wang et al., 2020a; Yu et al., 2020). In addition, many studies (Thornton et al., 2010;
78 Mielke et al., 2011; Phillips et al., 2012; Riedel et al., 2013; Bannan et al., 2015; Faxon et al., 2015;
79 Wang et al., 2017b; Wang et al., 2017c; Tham et al., 2018; Wang et al., 2018) have also reported
80 significant amounts of ClNO₂ at various continental sites with limited marine influence. For
81 example, ClNO₂ concentrations reached 4 ppbv in the summer of North China Plain (Tham et al.,
82 2016). These observations imply the importance of other sources for aerosol chloride, such as coal
83 combustion (Eger et al., 2019), biomass burning (Ahern et al., 2017), waste incineration (Bannan
84 et al., 2019), and snow-melting agent application (Mielke et al., 2016; McNamara et al., 2020).

85 In addition to insoluble minerals (e.g., quartz, feldspar, clay and carbonate), mineral dust
86 aerosols emitted from saline topsoil in arid and semi-arid regions may contain significant amounts
87 of soluble materials such as chloride and sulfate (Gillette et al., 1992; Abuduwailli et al., 2008;
88 Zhang et al., 2009; Wang et al., 2012; Jordan et al., 2015; Frie et al., 2017; Gaston et al., 2017;
89 Tang et al., 2019; Gaston, 2020). As elemental and mineralogical compositions are different for
90 conventional and saline mineral dust, they would differ significantly in physicochemical properties
91 and impacts on atmospheric chemistry and climate. For example, hygroscopicity and cloud
92 condensation nuclei (CCN) activities of saline mineral dust can be much higher than conventional



93 mineral dust (Pratt et al., 2010; Gaston et al., 2017; Tang et al., 2019; Zhang et al., 2020). Recent
94 laboratory studies (Mitroo et al., 2019; Royer et al., 2021) found that heterogeneous reactions of
95 N_2O_5 with saline mineral dust originating from western and southwestern USA can be very
96 effective and produce significant amounts of ClNO_2 . Large variations in $\gamma(\text{N}_2\text{O}_5)$ and $\varphi(\text{ClNO}_2)$
97 were reported (Mitroo et al., 2019; Royer et al., 2021), depending on RH as well as chemical and
98 mineralogical contents of saline mineral dust samples.

99 A very recent study (Wu et al., 2020) showed that N_2O_5 uptake onto saline mineral dust
100 contributed significantly to particulate nitrate formation during a dust storm event in Shanghai,
101 China. One may further expect that it may have a profound effect on ClNO_2 , especially considering
102 that vast areas in China are heavily affected by both mineral dust and NO_x . Nevertheless,
103 heterogeneous formation of ClNO_2 from N_2O_5 uptake onto saline mineral dust in other regions
104 rather than USA has not been explored. In order to provide key parameters required to assess the
105 potential of saline mineral dust as a ClNO_2 source in China, we conducted a series of laboratory
106 experiments to investigate ClNO_2 formation in heterogeneous reaction of N_2O_5 with several saline
107 mineral dust samples collected from different regions in China. In addition to difference in source
108 regions, saline mineral dust samples examined in our work have substantial variations in
109 composition and mineralogy, enabling us to examine the effects of particle composition and water
110 content on ClNO_2 production. In order to better understand variations of ClNO_2 yields with RH
111 and samples, we experimentally measured mass hygroscopic growth factors of the eight samples
112 examined, while previous studies (Mitroo et al., 2019; Royer et al., 2021) used the thermodynamic
113 model ISORROPIA-II (Fountoukis and Nenes, 2007) to predict particulate water contents. Based
114 on our laboratory results, we further use a 3-D chemical transport model (GEOS-Chem) to assess



115 the impacts of ClNO₂ produced from N₂O₅ uptake onto mineral dust on ClNO₂ and O₃ in China
116 during a major dust event which occurred in May 2017.

117 **2 Methodology**

118 **2.1 Characterization of saline mineral dust samples**

119 Eight saline mineral dust samples, originating from five different provinces in northern China
120 (including Ningxia, Xinjiang, Shandong, Inner Mongolia and Shaanxi), were examined in this
121 work, and full information of these samples can be found elsewhere (Tang et al., 2019). Table 1
122 summarizes key information of these samples. According to their chloride contents, the eight
123 samples were classified into three categories, including two high chloride samples (H1 and H2),
124 four medium chloride samples (M1, M2, M3 and M4) and two low chloride samples (L1 and L2).

125 Our previous work (Tang et al., 2019; Zhang et al., 2020) measured mass hygroscopic growth
126 factors of the eight samples at 0-90% RH with a RH resolution of 10%, using a vapor sorption
127 analyzer (Gu et al., 2017). As the highest RH at which heterogeneous reaction of N₂O₅ with saline
128 mineral dust was conducted in our work was ~75%, we further measured mass growth factors of
129 the eight samples at (75±2)% RH, and the results are also included in Table 1.

130

131 **Table 1.** Overview of mass fractions of major soluble ions and mass ratios of particulate water at
132 (75±2)% RH to dry particles for the eight saline mineral dust samples examined in this work. Mass
133 fractions of major soluble ions were reported previously (Tang et al., 2019), and particulate water
134 contents at (75±2)% RH were measured by the present work.

category	sample ^a	sample ^b	Na ⁺	Cl ⁻	SO ₄ ²⁻	H ₂ O (75%)
High Cl ⁻	H1	NX	0.3537	0.3870	0.0958	1.3093
	H2	XJ-5	0.2407	0.2145	0.0973	1.7066

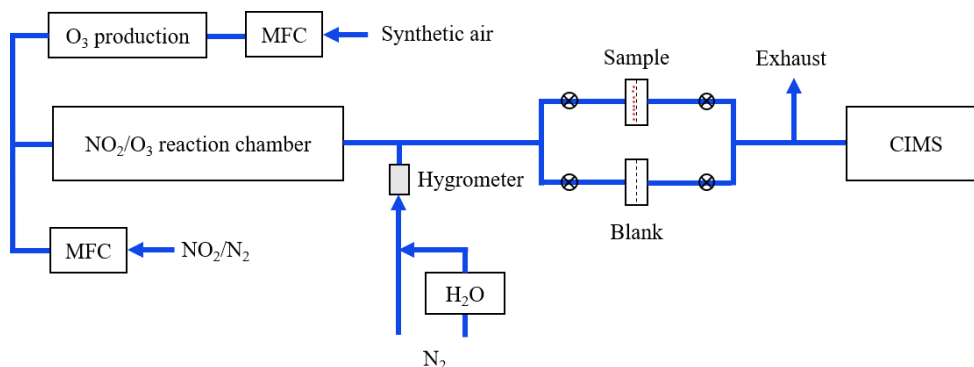


Medium Cl ⁻	M1	SD	0.0265	0.0508	0.0754	0.3911
	M2	XJ-4	0.0326	0.0341	0.0071	0.0428
	M3	IM-2	0.0471	0.0229	0.1413	0.2106
	M4	IM-3	0.1343	0.0095	0.3424	0.0174
Low Cl ⁻	L1	XJ-3	0.0239	0.0093	0.0497	0.0475
	L2	SX	0.0003	n.d.	n.d.	0.0126

135 ^a: sample names used in the present work; ^b:corresponding sample names used in our previous
136 work (Tang et al., 2019).

137 2.2 Experimental apparatus

138 Figure 1 shows the experimental apparatus used to study heterogeneous interactions of N₂O₅
139 with saline mineral dust. It mainly consists of three parts: 1) N₂O₅ generation, 2) gas-particle
140 interaction, and 3) detection of N₂O₅ and ClNO₂.



141

142 **Figure 1.** Schematic diagram of the experimental apparatus.

143 2.2.1 N₂O₅ generation

144 In our work, N₂O₅ was generated via oxidation of NO₂ by O₃. As shown in Figure 1, a
145 synthetic air flow (30 mL/min) was passed over a Hg lamp to produce O₃ via O₂ photolysis at
146 184.95 nm. The photolysis module was stabilized at 35±0.2 °C using a Peltier cooler controlled by
147 a Proportion Integration Differentiation (PID) algorithm, in order to give stable O₃ output. The



148 O₃/air flow was then mixed with a NO₂ flow (80 mL/min, 10 ppmv in synthetic air) in a
149 temperature-stabilized PFA reactor with a residence time of ~70 s to produce N₂O₅. After exiting
150 the PFA reactor, the flow (110 mL/min) was then diluted with a humidified nitrogen flow (2500
151 mL/min), and RH of the humidified nitrogen flow was monitored using a hygrometer. The final
152 flow had a total flow rate of 2610 mL/min, and initial N₂O₅ concentrations were in the range of
153 0.4-1.0 ppbv.

154 **2.2.2 Heterogeneous interactions**

155 As shown in Figure 1, the mixed flow (2610 mL/min) could be directed through a blank PTFE
156 membrane filter (47 mm, Whatman, USA) housed in a PFA filter holder, and in this case initial
157 N₂O₅ and ClNO₂ concentrations were measured. Alternatively, the flow could also be passed
158 through a PTFE filter loaded with saline mineral dust, and thus N₂O₅ and ClNO₂ concentrations
159 after heterogeneous reaction with saline mineral dust loaded on the filter were measured. During
160 our experiments, the flow could be switched back to pass through the blank filter in order to check
161 whether the initial N₂O₅ and ClNO₂ concentrations were stable.

162 Saline mineral dust particles were loaded onto PTFE filters using the method described in our
163 previous study (Li et al., 2020). PTFE filters were weighted before and after being loaded with
164 particles, in order to determine the mass of particles loaded onto these filters. In our work, the mass
165 of particles on filters were in range of 0.6-7.3 mg.

166 **2.2.3 Detection of N₂O₅ and ClNO₂**

167 After exiting one of the two filters, a flow of 2200 mL/min was sampled into a time-of-flight
168 chemical ionization mass spectrometry (TOF-CIMS) to measure N₂O₅ and ClNO₂ concentrations,
169 and the remaining flow (~400 mL/min) went into the exhaust. The CIMS instrument has been
170 detailed previously (Kercher et al., 2009; Wang et al., 2016). In brief, N₂O₅ and ClNO₂ were



171 detected as $\text{I}(\text{N}_2\text{O}_5)^-$ and $\text{I}(\text{ClNO}_2)^-$ clusters at 235 and 208 m/z (R2a, R2b) using I^- as the reagent
172 ion, and a soft X-ray device (Hamamatsu, Soft X-Ray 120°) was employed to generate I^- from
173 $\text{CH}_3\text{I}/\text{N}_2$. CIMS was calibrated before and after our experiments which lasted for ~1 month, and
174 further details on calibration can be found in the Appendix.



177 **2.3 Model description**

178 We use GEOS-Chem (version 12.9.3) to quantify the effects of ClNO_2 formation due to
179 heterogeneous reaction of N_2O_5 with saline dust in China. The model, which includes a detailed
180 representation of coupled ozone- NO_x -VOCs-aerosol-halogen chemistry (Wang et al., 2021), is
181 driven by MERRA2 (the Modern-Era Retrospective Analysis for Research and Applications,
182 Version 2) assimilated meteorological fields from the NASA Global Modeling and Assimilation
183 Office (GMAO) with native horizontal resolution of $0.25^\circ \times 0.3125^\circ$ and 72 vertical levels from the
184 surface to the mesosphere. Our simulation was conducted over East Asia (60° - 150°E , 10°S - 55°N)
185 at the native resolution with dynamical boundary conditions from a $4^\circ \times 5^\circ$ global simulation.
186 Anthropogenic emissions in China are based on the Multiresolution Emission Inventory for China
187 (MEIC) (Zheng et al., 2018) and an inventory of HCl and fine particulate Cl^- in China (Fu et al.,
188 2018). Natural dust emissions are calculated based on Ridley et al. Ridley et al. (2013). A more
189 detailed description of the model and emissions can be found elsewhere (Wang et al., 2020b).

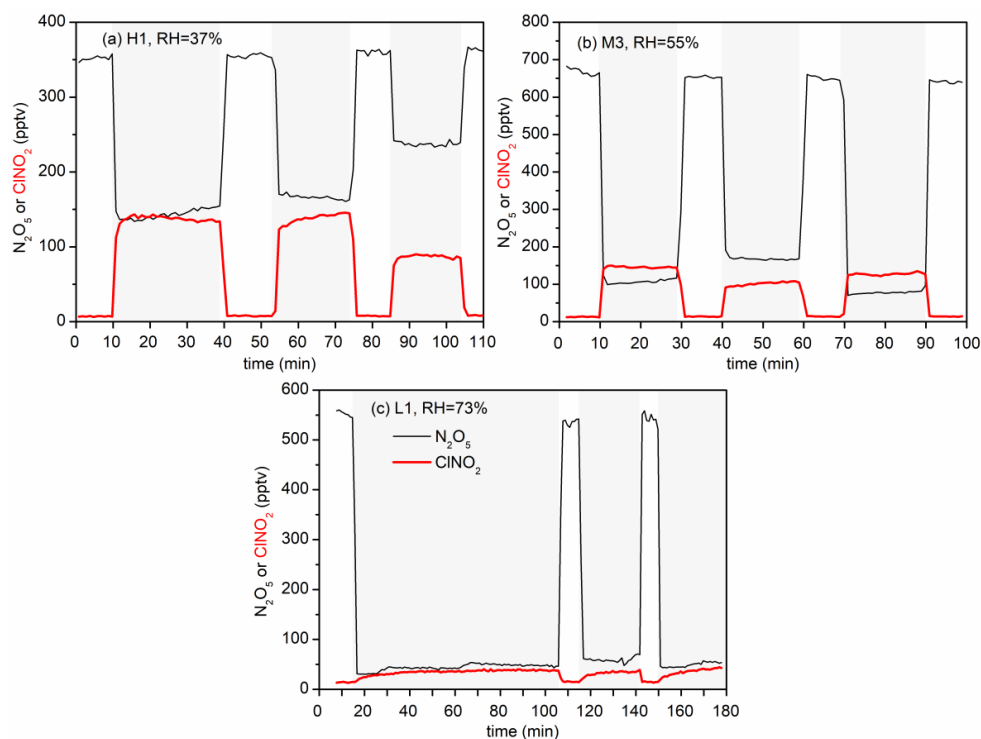
190 For N_2O_5 uptake onto aqueous aerosols, the parameterization in our previous study (Wang et
191 al., 2020b) for $\gamma(\text{N}_2\text{O}_5)$ and $\varphi(\text{ClNO}_2)$, which are based on a detail evaluation of different model
192 parameterizations by previous work (McDuffie et al., 2018a; McDuffie et al., 2018b), is used in
193 this study. For N_2O_5 uptake on dust aerosol, $\gamma(\text{N}_2\text{O}_5)$ is always assumed to be 0.02, as



194 recommended previously (Crowley et al., 2010; Tang et al., 2017), and $\phi(\text{ClNO}_2)$ is assumed to
195 be 0 in the standard case, i.e., no ClNO_2 is produced in heterogeneous reaction of N_2O_5 with
196 mineral dust.

197 **3 Results and discussion**

198 Figure 2a shows changes in N_2O_5 and ClNO_2 concentrations during an experiment in which
199 heterogeneous reaction of N_2O_5 with sample H1 at 37% RH was studied. As shown in Figure 2a,
200 when the mixed flow was passed through the blank filter (0-10 min), N_2O_5 concentrations were
201 measured to be ~ 350 pptv and ClNO_2 was below the detection limit. The mixed flow was then
202 passed through the particle-loaded filter at ~ 10 min in order to initiate heterogeneous reaction of
203 N_2O_5 with sample H1, and significant decrease in N_2O_5 concentrations (from ~ 350 to ~ 150 pptv)
204 and increase in ClNO_2 concentrations (from almost 0 to ~ 150 pptv) were observed, suggesting that
205 heterogeneous interaction with sample H1 substantially consumed N_2O_5 and generated ClNO_2 . In
206 order to check if initial N_2O_5 and ClNO_2 concentrations were stable, during our experiments the
207 mixed flow was switched back to pass through the blank filter from time to time (e.g., at around
208 40, 75 and 105 min for the experiment displayed in Figure 2a). Indeed, initial N_2O_5 and ClNO_2
209 concentrations were constant in our experiments, with another two examples shown in Figures 2b
210 and 2c.



211

212 **Figure 2.** Time series for measured N_2O_5 and ClNO_2 concentrations after the mixed flow was
213 passed through the blank filter or the particle-loaded filter: a) H1, 37% RH; b) M3, 55% RH; c)
214 L1, 73% RH. Periods in which the mixed flow was passed through the particle-loaded filter was
215 shadowed with gray.

216

217 Figures 2b and 2c show time series of measured N_2O_5 and ClNO_2 concentrations in another
218 two experiments, suggesting that heterogeneous reaction with sample M3 and L1 also led to
219 substantial removal of N_2O_5 . However, much less ClNO_2 was produced for sample M3 and L1,
220 when compared to sample H1 (Figure 2a). The decrease in N_2O_5 concentrations, $\Delta[\text{N}_2\text{O}_5]$, and the
221 increase in ClNO_2 concentrations, $\Delta[\text{ClNO}_2]$, can be used to calculate ClNO_2 yields, $\varphi(\text{ClNO}_2)$,
222 according to Eq. (1).



223
$$\varphi(\text{ClNO}_2) = \frac{\Delta[\text{ClNO}_2]}{\Delta[\text{N}_2\text{O}_5]} \quad (1)$$

224 In this work we measured $\varphi(\text{ClNO}_2)$ for heterogeneous reaction of N_2O_5 with eight different
225 saline mineral dust samples at four RH, and each experiment was repeated at least three times. It
226 should be mentioned that during each experiment the measured $\varphi(\text{ClNO}_2)$ did not vary
227 significantly with time, and therefore an average value of $\varphi(\text{ClNO}_2)$ was reported for each
228 experiment. Table 2 summarizes measured $\varphi(\text{ClNO}_2)$ for the eight samples at different RH, and
229 the results are further discussed in the following sections.

230

231 **Table 2.** Measured ClNO_2 yields for heterogeneous uptake of N_2O_5 onto saline mineral dust
232 samples at different RH. All the errors given in this work are standard deviations. The uncertainty
233 of RH was $\pm 2\%$.

sample	18% RH	36% RH	56% RH	75% RH
H1	0.402±0.138	0.663±0.039	0.774±0.028	0.697±0.311
H2	0.560±0.046	0.474±0.026	0.494±0.042	0.378±0.069
M1	0.271±0.038	0.271±0.030	0.418±0.053	0.543±0.086
M2	0.166±0.018	0.246±0.041	0.316±0.046	0.418±0.052
M3	0.223±0.061	0.251±0.050	0.211±0.025	0.120±0.050
M4	0.179±0.075	0.133±0.007	0.205±0.021	0.181±0.044
L1	0.037±0.006	0.030±0.015	0.045±0.025	0.048±0.008
L2	0.012±0.003	0.005±0.004	0.024±0.042	0.041±0.039

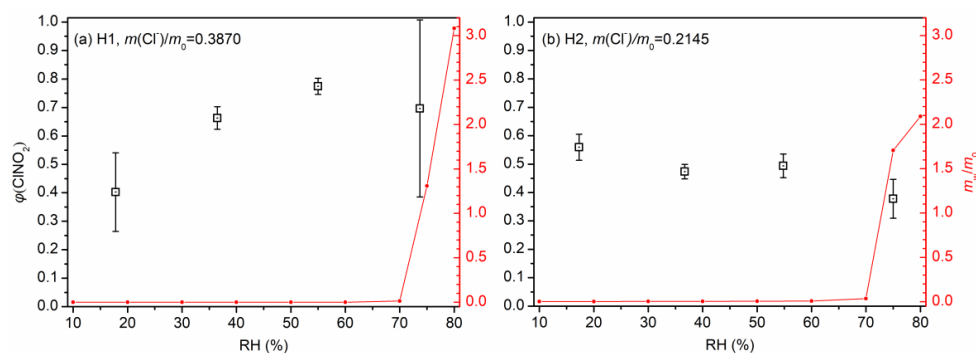
234

235 3.1 ClNO_2 production yields

236 Figure 3 shows ClNO_2 yields as a function of RH for the two samples with high chloride
237 content (H1 and H2), and $\varphi(\text{ClNO}_2)$ were found to be quite high for the two samples. To be more
238 specific, the mass fraction of chloride was 0.3870 for sample H1, and $\varphi(\text{ClNO}_2)$ were found to
239 increase from 0.402±0.138 at 18% RH to 0.774±0.028 at 56% RH, and then slightly decreased to



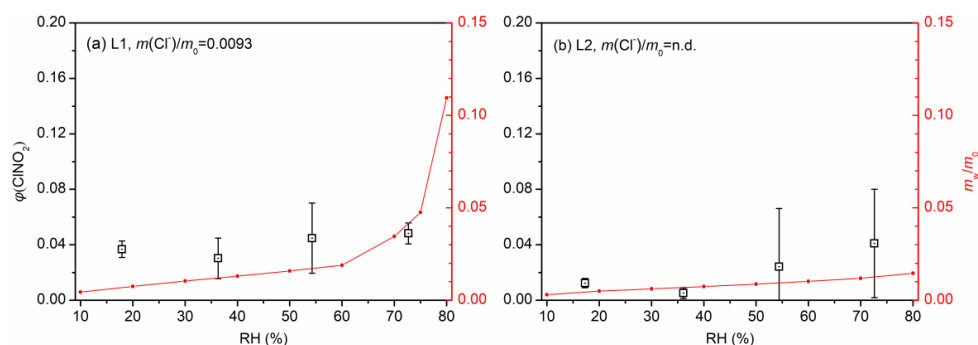
240 0.697 ± 0.311 when RH was further increased to 75%. For sample H2, the mass fraction of chloride
241 (0.2145) was lower than sample H1, and $\varphi(\text{ClNO}_2)$ showed a small decrease (or remained
242 relatively constant) when RH was increased from 18% to 56%, ranging from 0.474 ± 0.026 to
243 0.560 ± 0.046 ; further increase in RH to 75% resulted in small decrease in $\varphi(\text{ClNO}_2)$ to 0.378 ± 0.069 .



244
245 **Figure 3.** Measured ClNO_2 yields (black symbol) and normalized mass (normalized to the mass
246 of dry particles) of particulate water (red line) as a function of RH for (a) H1 and (b) H2. The error
247 bar represents standard deviation.

248

249 ClNO_2 yields are shown in Figure 4 as a function of RH for the two low chloride samples (L1
250 and L2), and their mass fractions of chloride were < 0.01 . As shown in Figure 4, $\varphi(\text{ClNO}_2)$ were
251 found to be always < 0.05 for the two samples, suggesting that heterogeneous production of ClNO_2
252 was very limited, despite substantial removal of N_2O_5 due to heterogeneous reaction (with an
253 example shown in Figure 2c). The low $\varphi(\text{ClNO}_2)$ values for sample L1 and L2 could be attributed
254 to their low chloride contents. In addition, $\varphi(\text{ClNO}_2)$ appeared to increase with RH for L1 and L2;
255 however, since the uncertainties associated with $\varphi(\text{ClNO}_2)$ were rather large for these two samples,
256 the dependence of $\varphi(\text{ClNO}_2)$ on RH should be treated in caution.

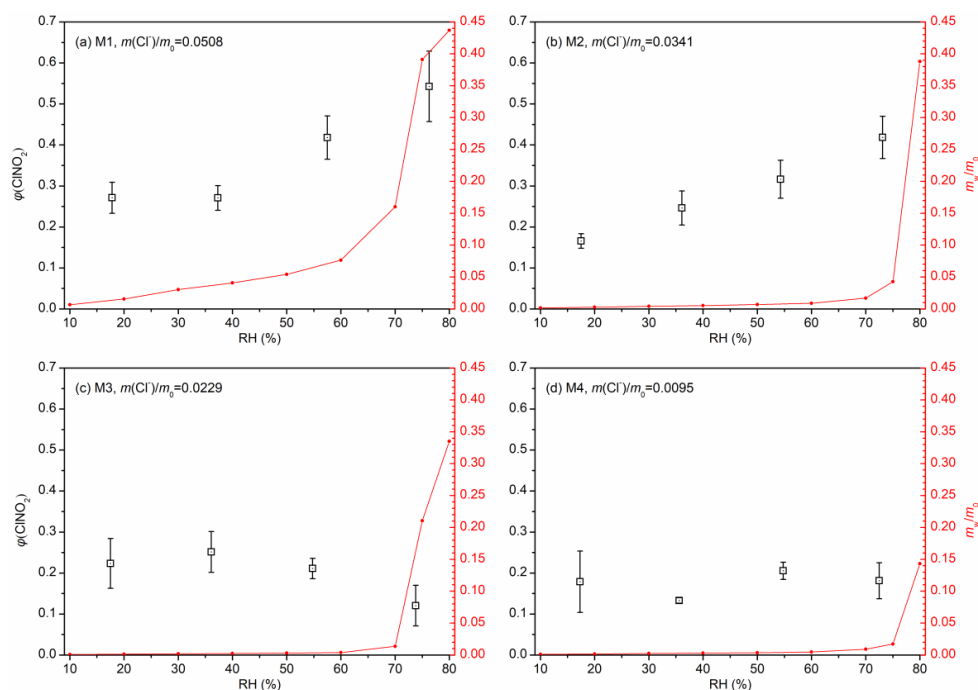


257

258 **Figure 4.** Measured ClNO_2 yield (black symbol) and normalized mass (normalized to the mass of
259 dry particles) of particulate water (red line) as a function of RH for (a) L1 and (b) L2 (n. d.: not
260 detected). The error bar represents standard deviation.

261

262 We also investigated ClNO_2 production from heterogeneous reaction of N_2O_5 with four
263 samples with medium chloride contents (M1, M2, M3 and M4), and the results are displayed in
264 Figure 5. Mass fractions of chloride were determined to be 0.0508 for M1, 0.034 for M2, 0.0229
265 for M3 and 0.0095 for M4, respectively. ClNO_2 yields were found to increase significantly with
266 RH for M1 and M2; more specifically, $\varphi(\text{ClNO}_2)$ increased from 0.271 ± 0.038 at 18% RH to
267 0.543 ± 0.086 at 75% RH for sample M1, and increased from 0.166 ± 0.018 at 18% RH to
268 0.418 ± 0.0052 at 75% RH for sample M2. As shown in Figure 5, the dependence of $\varphi(\text{ClNO}_2)$ on
269 RH for the other two medium chloride samples (M3 and M4) were rather different from M1 and
270 M2. For sample M3, $\varphi(\text{ClNO}_2)$ first increased from 0.223 ± 0.061 at 18% RH to 0.251 ± 0.050 at 36%
271 RH, and further increase in RH to 75% caused substantial reduction in $\varphi(\text{ClNO}_2)$. At last, no
272 significant variation of $\varphi(\text{ClNO}_2)$ with RH (18-75%) was observed for sample M4.



273

274 **Figure 5.** Measured CINO₂ yield (black symbol) and normalized mass (normalized to the mass of
275 dry particles) of particulate water (red line) as a function of RH for (a) M1, (b) M2, (c) M3, and
276 (d) M4. The error bar represents standard deviation.

277 3.2 The effects of RH

278 The dependence of $\varphi(\text{ClNO}_2)$ on RH for the eight saline mineral samples we examined, as
279 discussed in Section 3.1, exhibited two interesting features. First, when RH was as low as 18%,
280 large $\varphi(\text{ClNO}_2)$ values (>0.2) were observed for four samples (H1, H2, M1 and M3). As the
281 deliquescence RH of NaCl is $\sim 75\%$, one may wonder where aqueous chloride, which is necessary
282 for heterogeneous formation of CINO₂, came from at 18% RH. As initially suggested by a previous
283 study (Mitroo et al., 2019), the occurrence of aqueous chloride in saline mineral dust particles at
284 low RH could be due to the presence of CaCl₂ and MgCl₂, which were amorphous under dry
285 conditions and could take up water at very low RH (Guo et al., 2019). Our previous study (Tang



286 et al., 2019) measured water soluble ions contained by the eight saline mineral dust samples, and
287 the amounts of water soluble Ca^{2+} and Mg^{2+} in the four samples (H1, H2, M1 and M3) with larger
288 $\varphi(\text{ClNO}_2)$ at 18% RH were significantly larger than those in the other four samples (M2, M4, L1
289 and L2). This observation further supported our deduction that the presence of CaCl_2 and MgCl_2
290 enabled efficient formation of ClNO_2 at low RH.

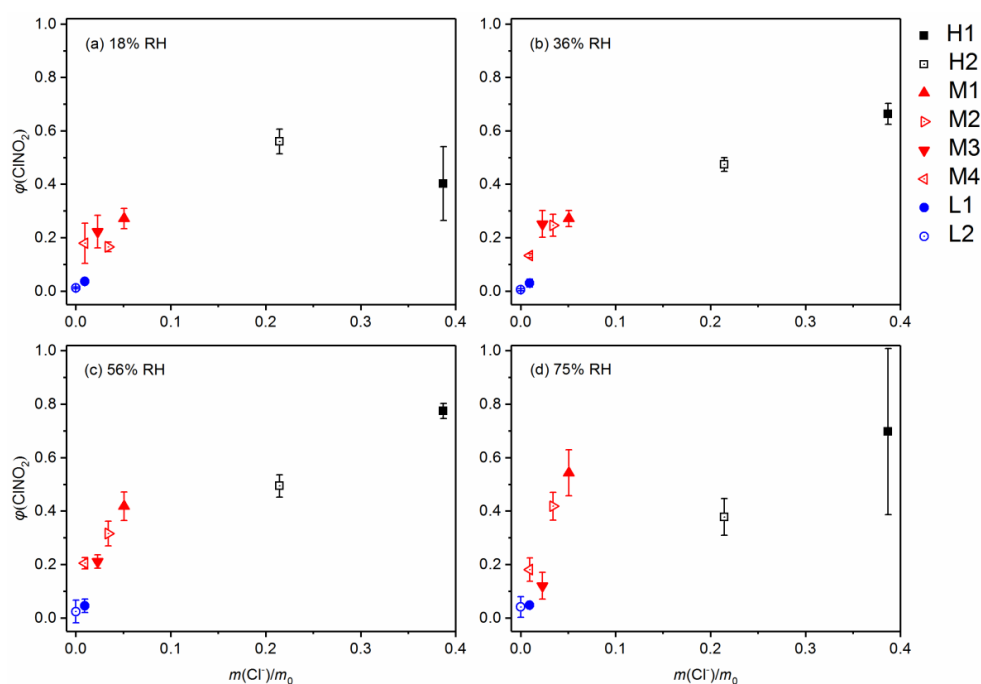
291 The second interesting feature is that as shown in Figures 3-5, $\varphi(\text{ClNO}_2)$ could increase,
292 decrease or remain relatively constant with increase in RH from 18% to 75%. This feature can be
293 understood given the complex mechanisms driving heterogeneous uptake of N_2O_5 onto saline
294 mineral dust (Mitroo et al., 2019; Royer et al., 2021): at a given RH, N_2O_5 can react with aqueous
295 water, aqueous chloride and insoluble minerals, and only its reaction with aqueous chloride would
296 produce ClNO_2 . The possible effects of RH on $\varphi(\text{ClNO}_2)$ are discussed below: 1) as RH increases,
297 heterogeneous reactivity of N_2O_5 towards insoluble minerals can be enhanced, suppressed or
298 remain largely unchanged (Tang et al., 2012; Tang et al., 2017); 2) increase in RH would lead to
299 further hygroscopic growth and dilution of aqueous solutions, leading to decrease in $\varphi(\text{ClNO}_2)$ in
300 this aspect; 3) the increase in particulate water with RH would cause more chloride to be dissolved
301 into aqueous solutions, and in this aspect increase in RH would promote ClNO_2 formation. As a
302 result, it is not surprised to observe different dependence of $\varphi(\text{ClNO}_2)$ on RH for different saline
303 mineral dust samples.

304 3.3 Discussion

305 Figure 6 shows the dependence of $\varphi(\text{ClNO}_2)$ on mass fractions of chloride for the eight
306 samples we examined at four different RH. These samples showed significant variation in
307 $\varphi(\text{ClNO}_2)$, ranging from <0.1 to >0.7 , and $\varphi(\text{ClNO}_2)$ were largest for the two high chloride samples
308 (H1 and H2), followed by median (M1, M2, M3 and M4) and low chloride samples (L1 and L2).



309 Overall, a positive dependence of $\varphi(\text{ClNO}_2)$ on mass fractions of chloride was observed at each
310 RH. Figure 6 also reveals that the measured $\varphi(\text{ClNO}_2)$ were very sensitive to mass fractions of
311 chloride when the mass fractions of chloride were below 10%. However, as shown in Figure 6,
312 higher chloride contents did not always mean larger $\varphi(\text{ClNO}_2)$, and similar observations were also
313 reported by previous work (Mitroo et al., 2019; Royer et al., 2021).



314

315 **Figure 6.** Dependence of ClNO_2 yields on mass fractions of chloride for the eight saline mineral
316 dust samples at a given RH: a) 18% RH; b) 36% RH; c) 56% RH; d) 75% RH.

317

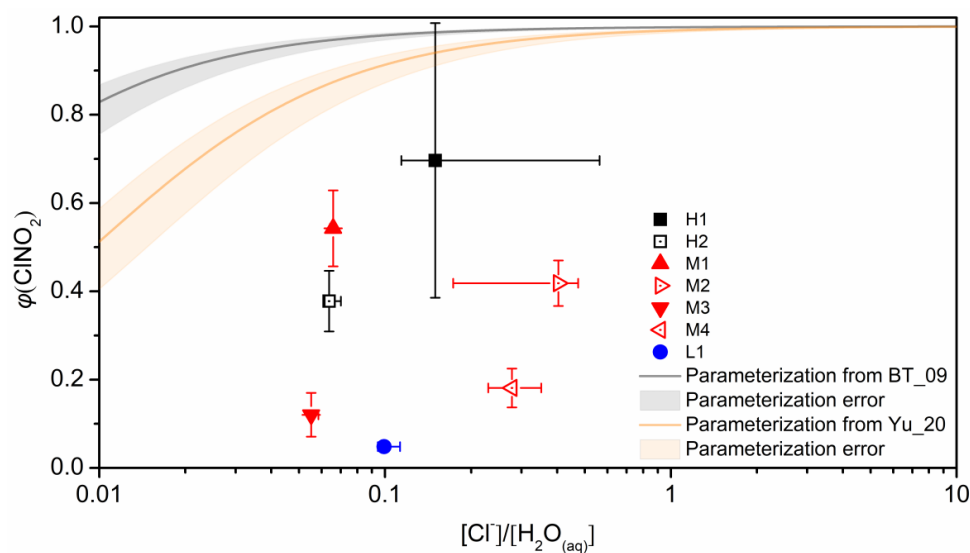
318 Two parameterizations have been widely used to predict the dependence of $\varphi(\text{ClNO}_2)$ on
319 chemical compositions and water contents of aqueous aerosol particles (Bertram and Thornton,
320 2009; Yu et al., 2020). Based on laboratory results, Bertram and Thornton (2009) suggested that
321 ClNO_2 yields can be calculated using Eq. (2):



322
$$\varphi(\text{ClNO}_2) = \left(1 + \frac{k(\text{H}_2\text{O}) \cdot [\text{H}_2\text{O}_{(\text{aq})}]}{k(\text{Cl}^-) \cdot [\text{Cl}^-]}\right)^{-1} \quad (2)$$

323 where $[\text{H}_2\text{O}_{(\text{aq})}]/[\text{Cl}^-]$ is the ratio of molar concentration of H_2O to that of Cl^- in aqueous particles,
324 and the value of $k(\text{H}_2\text{O})/k(\text{Cl}^-)$ was suggested to be $1/(483 \pm 175)$ (Bertram and Thornton, 2009).
325 Very recently, Yu et al. (2020) examined uptake coefficients of N_2O_5 onto ambient aerosol
326 particles at four different sites in China, and suggested that using a value of $1/(105 \pm 37)$ for
327 $k(\text{H}_2\text{O})/k(\text{Cl}^-)$ would lead to better agreement between measured and predicted uptake coefficients
328 of N_2O_5 (Yu et al., 2020).

329 The two parameterizations were used in our work to calculate $\varphi(\text{ClNO}_2)$ at 75% RH for the
330 eight saline mineral dust samples we examined. $[\text{H}_2\text{O}_{(\text{aq})}]/[\text{Cl}^-]$ was calculated from the measured
331 mass growth factors at 75% RH and the mass fractions of chloride, assuming that all the chloride
332 contained by saline mineral dust samples was dissolved into aqueous solutions at 75% RH. The
333 comparison between measured and calculated $\varphi(\text{ClNO}_2)$ is displayed in Figure 7, suggesting that
334 both parameterizations significantly overestimated the measured $\varphi(\text{ClNO}_2)$ for all the eight saline
335 mineral dust samples we investigated. A previous study (Mitroo et al., 2019) investigated $\varphi(\text{ClNO}_2)$
336 for heterogeneous uptake of N_2O_5 onto saline mineral dust samples collected in southwestern USA,
337 and similarly they found that the measured $\varphi(\text{ClNO}_2)$ were significantly smaller than those
338 predicted using the parameterization proposed by Bertram and Thornton (2009).



339
340 **Figure 7.** Measured and calculated of $\varphi(\text{ClNO}_2)$ at $75 \pm 2\%$ RH as a function of $[\text{Cl}^-]/[\text{H}_2\text{O}_{(\text{aq})}]$.
341 Black and orange curves represent $\varphi(\text{ClNO}_2)$ calculated using the BT_09 parameterization
342 (Bertram and Thornton, 2009) and the Yu_20 parameterization (Yu et al., 2020), and the associated
343 errors are represented by the corresponding shadows.

344

345 The observed discrepancies between measured and predicted $\varphi(\text{ClNO}_2)$ can be caused by
346 several reasons. First, even at $\sim 75\%$ RH (the highest RH at which our experiments were conducted),
347 chloride contained in saline mineral dust may not be fully dissolved, and therefore our calculation
348 may overestimate $[\text{Cl}^-]/[\text{H}_2\text{O}_{(\text{aq})}]$ and thus also overestimate $\varphi(\text{ClNO}_2)$. Second, perhaps more
349 importantly, saline mineral dust samples contain substantial amounts of insoluble minerals, and
350 some of these minerals, such as clays, are very reactive towards N_2O_5 (Tang et al., 2017); however,
351 the two parameterizations did not take into account heterogeneous reaction of N_2O_5 with insoluble
352 minerals, and as a result would inevitably overestimate $\varphi(\text{ClNO}_2)$. At last, our calculations
353 assumed internal mixing, but inter- and intra-particle heterogeneity of saline mineral dust particles
354 could also contribute to the observed gap between measured and calculated $\varphi(\text{ClNO}_2)$. For



355 example, a wintertime field campaign at Ann Arbor (Michigan, USA) (McNamara et al., 2020)
356 showed that nonhomogeneous chloride distribution across road salt aerosol particles would result
357 in significant overestimation of $\varphi(\text{ClNO}_2)$. The comparison between measured and predicted
358 $\varphi(\text{ClNO}_2)$ suggested that while heterogeneous uptake of N_2O_5 onto saline mineral dust could be
359 an important source of inland ClNO_2 , underlying mechanisms which affect heterogeneous
360 production of ClNO_2 from saline mineral dust have not been well elucidated.

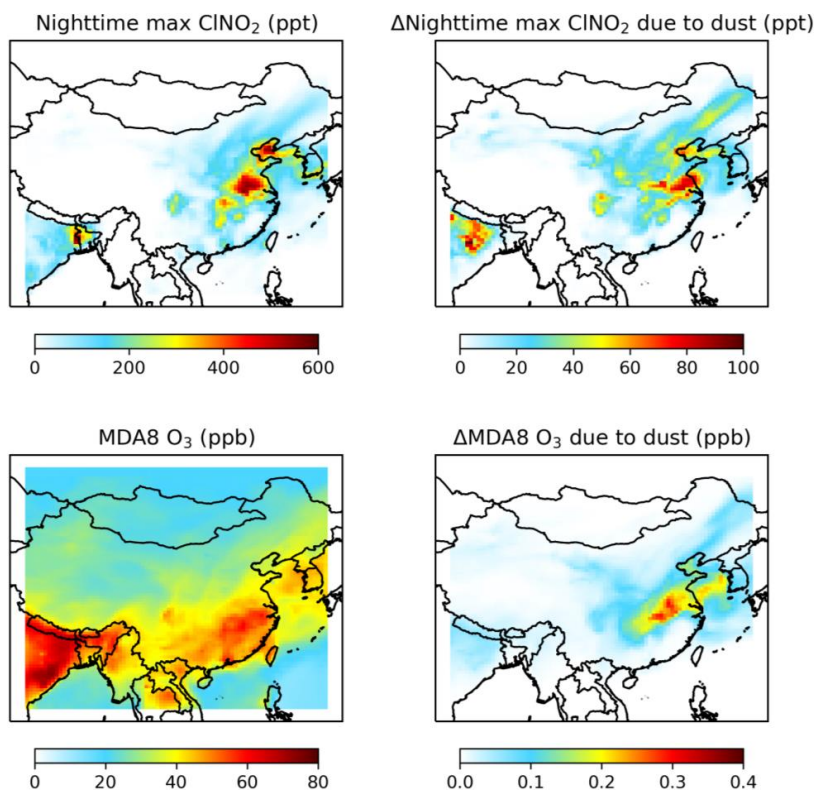
361 **4 Atmospheric implications**

362 We consider ClNO_2 formation in heterogeneous uptake of N_2O_5 onto dust aerosol in GEOS-
363 Chem to explore its implications. Since Cl^- concentration in mineral dust is not well known and
364 currently we are not able to parameterize $\varphi(\text{ClNO}_2)$ for mineral dust (as discussed in Section 3.3),
365 we use a fixed $\varphi(\text{ClNO}_2)$ value of 0.1 in our simulation. This value is higher than those determined
366 in our work for low chloride samples but lower than those for medium chloride samples. We focus
367 on simulations on 2-7 May 2017, during which a large dust event took place in East Asia. It caused
368 high concentrations of dust aerosols with maximum hourly concentration higher than $1000 \mu\text{g}/\text{m}^3$
369 over a wide area in China (Zhang et al., 2018), which are also well captured by our simulations
370 (Figure S1).

371 Figure 8 shows the weekly mean values of the nighttime maximum surface ClNO_2 mixing
372 ratios and the contribution of heterogeneous reaction of N_2O_5 with dust aerosol to ClNO_2 over 2-
373 7 May 2017. The impact of N_2O_5 uptake onto dust aerosol is calculated as the difference between
374 the standard case in which $\varphi(\text{ClNO}_2)$ is assumed to be 0 for N_2O_5 uptake onto dust aerosol and the
375 case in which $\varphi(\text{ClNO}_2)$ is assumed to be 0.1. Due to large diurnal variations and near-zero mixing
376 ratios of ClNO_2 in the daytime, we use the mean nighttime maximum value for ClNO_2 , following
377 previous standard practice (Wang et al., 2019). The largest impact on ClNO_2 is found in Central



378 China, where weekly mean nighttime maximum surface ClNO_2 mixing ratios are increased by 85
379 pptv, due to heavy impact of dust aerosol transported from the north and high NO_x emissions in
380 this region. Even larger effects (up to 240 pptv increase in ClNO_2) can be found on some individual
381 days, as shown in Figures S2 and S3. These results suggest that N_2O_5 uptake onto dust could be
382 an important source for tropospheric ClNO_2 over Central and Northeast China, where ClNO_2
383 formation is conventionally believed to be limited due to relatively low aerosol chloride levels
384 from sea salts and anthropogenic sources.



385
386 **Figure 8.** Modeled weekly mean mixing ratios of nighttime maximum ClNO_2 (upper panels) and
387 maximum daily 8-h average (MDA8) ozone (bottom panels) in surface air over China during 2-7
388 May 2017. The left panels show simulated mixing ratios in our standard case in which $\phi(\text{ClNO}_2)$



389 is assumed to be 0 for N_2O_5 uptake onto dust aerosol. The right panels show impacts of ClNO_2
390 formation due to N_2O_5 uptake onto dust, calculated as the difference between the standard case
391 and the case in which $\varphi(\text{ClNO}_2)$ is assumed to be 0.1 for N_2O_5 uptake onto dust.

392

393 Figure 8 also shows the effect of ClNO_2 formation due to heterogeneous reaction of N_2O_5
394 with dust aerosol on the daily maximum 8-h average (MDA8) ozone mixing ratios in the surface
395 air over China during the same period. MDA8 ozone mixing ratios are increased by up to 0.32
396 ppbv after considering mineral dust as an additional source of ClNO_2 . Our simulation assumes a
397 low value of $\varphi(\text{ClNO}_2)$ in our measured range (<0.05 to ~ 0.77), and is conducted in summer when
398 ClNO_2 is more difficult to be accumulated due to short night. We expect that its impacts on ClNO_2
399 and ozone could be larger for dust events in winter and spring.

400 **5 Conclusions**

401 It has been widely recognized that nitryl chloride (ClNO_2), produced by heterogeneous
402 reaction of N_2O_5 with chloride-containing aerosols, could significantly affect atmospheric
403 oxidation capacity. However, heterogeneous formation of tropospheric ClNO_2 in inland regions in
404 China has not been well elucidated. In this work, we investigated ClNO_2 formation in
405 heterogeneous reaction of N_2O_5 with eight saline mineral dust samples collected from different
406 regions in China as a function of RH (18-75%). Significant production of ClNO_2 was observed for
407 some of the saline mineral dust samples examined, and ClNO_2 yields, $\varphi(\text{ClNO}_2)$, were determined
408 to span from <0.05 to 0.77, depending on chemical compositions of saline mineral dust samples
409 and RH. In general a positive dependence of $\varphi(\text{ClNO}_2)$ on mass fractions of particulate chloride
410 was observed at each RH, but higher particulate chloride content did not always mean larger
411 $\varphi(\text{ClNO}_2)$. On the other hand, increase in RH could increase, reduce or have no significant impacts



412 on $\varphi(\text{ClNO}_2)$, revealing the complex mechanisms which drive heterogeneous uptake of N_2O_5 onto
413 saline mineral dust.

414 Two widely-used parameterizations (Bertram and Thornton, 2009; Yu et al., 2020) were used
415 to estimate $\varphi(\text{ClNO}_2)$ at 75% RH for the eight saline mineral dust samples we investigated. Both
416 parameterizations were found to significantly overestimate the measured $\varphi(\text{ClNO}_2)$, and we
417 suggested that the discrepancies between measured and predicted $\varphi(\text{ClNO}_2)$ could be due to
418 incomplete dissolution of particulate chloride, heterogeneous reaction of N_2O_5 with insoluble
419 minerals, and/or inter- and intra-particle heterogeneity of saline mineral dust particles.

420 Assuming a $\varphi(\text{ClNO}_2)$ value of 0.1 for heterogeneous reaction of N_2O_5 with mineral dust, we
421 use GEOS-Chem to assess the impact of this reaction on tropospheric ClNO_2 and O_3 in China
422 during a severe dust event on 2-7 May 2017. It is found that after taking into ClNO_2 production
423 due to N_2O_5 uptake onto mineral dust aerosol, weekly mean nighttime maximum ClNO_2 mixing
424 ratios could be increased by up to 85 pptv during this period and the daily maximum 8-h average
425 O_3 mixing ratios were increased by up to 0.32 ppbv.

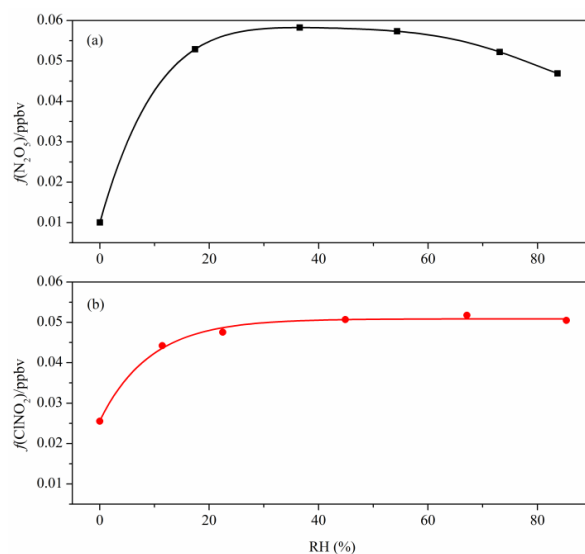
426 In summary, our work shows that heterogeneous reaction of N_2O_5 with saline mineral dust
427 can be an important source for tropospheric ClNO_2 in inland China. This reaction may also
428 important for tropospheric ClNO_2 production in many other regions over the world, as the
429 occurrence of saline mineral dust aerosols has been reported in various locations, such as Iran
430 (Gholampour et al., 2015), United States (Blank et al., 1999; Pratt et al., 2010; Jordan et al., 2015;
431 Frie et al., 2017), and Argentina (Bucher and Stein, 2016). Currently our limited knowledge
432 precludes quantitative prediction of heterogeneous ClNO_2 production from saline mineral dust,
433 and further investigation is thus warranted.

434



435 **Appendix. N₂O₅ and ClNO₂ calibration**

436 To calibrate CIMS measurements of N₂O₅, a mixed flow containing N₂O₅, which was
437 produced via O₃ oxidation of NO₂, was sampled into the CIMS instrument, and N₂O₅ was
438 quantified using the normalized intensities of I(N₂O₅)⁻ clusters, $f(\text{N}_2\text{O}_5)$, defined as the ratio of
439 signal intensity (cps) of I(N₂O₅)⁻ to that of the total reagent ions, i.e. I⁻ and I(H₂O)⁻. N₂O₅
440 concentrations in the mixed flow were quantified using cavity-enhanced absorption spectroscopy
441 (CEAS) (Wang et al., 2017a), with a detection limit of 2.7 pptv in 5 s and an uncertainty of ~25%.
442 RH of the mixed flow was varied during the calibration in order to determine the CIMS sensitivity
443 for N₂O₅ at different RH, and the results are displayed in Figure A1. The sensitivity for N₂O₅ first
444 increased with RH, reaching the maximum value at ~40% RH, and then decreased with further
445 increase in RH.



446

447 **Figure A1.** CIMS sensitivities as a function of RH for (a) N₂O₅ and (b) ClNO₂.

448



449 To calibrate CIMS measurements of ClNO₂, a nitrogen flow (6 mL/min) containing 10 ppmv
450 Cl₂ was passed over a slurry containing NaNO₂ and NaCl to produce ClNO₂ (Thaler et al., 2011),
451 and NaCl was included in the slurry in order to minimize the formation of NO₂ as a byproduct.
452 The mixed flow containing ClNO₂ was then conditioned to a given RH and sampled into the CIMS
453 instrument; similar to N₂O₅, ClNO₂ was quantified using the normalized intensities of I(ClNO₂)⁻
454 clusters, $f(\text{ClNO}_2)$, defined as the ratio of signal intensity (cps) of I(ClNO₂)⁻ to that of the total
455 reagent ions. To quantify ClNO₂, the mixed flow was delivered directly into a cavity attenuated
456 phase shift spectroscopy instrument (CAPS, Model N500, Teledyne API) to measure background
457 NO₂ concentrations; after that, the mixed flow was delivered through a thermal dissociation model
458 at 365 °C to fully decompose ClNO₂ to NO₂, and the total NO₂ concentrations were then
459 determined using CAPS. The differences in the measured NO₂ concentrations with and without
460 thermal dissociation was equal to ClNO₂ concentrations. The CAPS instrument had a detection
461 limit of 0.2 ppbv in 1 min for NO₂ and an uncertainty of ~10%. As shown in Figure A1, the
462 sensitivity for ClNO₂ increased with RH up to 40%, and showed little variation with further
463 increase in RH.

464 The detection limits of CIMS were 2 pptv for N₂O₅ and 3 pptv for ClNO₂, calculated as four
465 times of standard deviations (4σ) when measuring blank samples with 1 min average, and the
466 accuracy was estimated to be ~25%.

467



468 **Data availability**

469 Data used in this paper can be found in the main text or supplement. GEOS-Chem model is
470 available at GEOS-Chem repository (<http://www.geos-chem.org>).

471 **Competing interests**

472 The authors declare that they have no conflict of interest.

473 **Author contribution**

474 **Haichao Wang:** investigation, formal analysis, writing-original draft, writing – review & editing;

475 **Chao Peng:** investigation, formal analysis, writing-original draft, writing – review & editing;

476 **Xuan Wang:** investigation, formal analysis, writing-original draft, writing – review & editing;

477 **Shengrong Lou:** resources; **Keding Lu:** resources, supervision; **Guicheng Gan:** investigation;

478 **Xiaohong Jia:** investigation; **Xiaorui Chen:** investigation; **Jun Chen:** supervision; **Hongli Wang:**

479 resources; **Shaojia Fan:** resources; **Xinming Wang:** resources; **Mingjin Tang:** conceptualization,

480 formal analysis, resources, supervision, writing-original draft, writing-review & editing.

481 **Financial support**

482 This work was funded by National Natural Science Foundation of China (41907185, 91744204

483 and 42022050), Ministry of Science and Technology of China (2018YFC0213901), Guangdong

484 Basic and Applied Basic Research Fund Committee (2020B1515130003), National State

485 Environmental Protection Key Laboratory of Formation and Prevention of Urban Air Pollution

486 Complex (CX2020080094 and CX2020080578), Guangdong Foundation for Program of Science

487 and Technology Research (2019B121205006 and 2020B1212060053), Guangdong Science and

488 Technology Department (2017GC010501) and CAS Pioneer Hundred Talents program.

489



490 Reference

- 491 Abuduwailli, J., Gabchenko, M. V., and Xu, J.: Eolian transport of salts - A case study in the area
492 of Lake Ebinur (Xinjiang, Northwest China), *Journal of Arid Environments*, 72, 1843-1852,
493 2008.
- 494 Ahern, A., Goldberger, L., Jahl, L., Thornton, J., and Sullivan, R. C.: Production of N₂O₅ and
495 ClNO₂ through nocturnal processing of biomass-burning aerosol, *Environmental science &
496 technology*, 52, 550-559, 2017.
- 497 Atkinson, R., and Arey, J.: Atmospheric degradation of volatile organic compounds, *Chemical
498 Reviews*, 103, 4605-4638, 2003.
- 499 Atkinson, R., Baulch, D. L., Cox, R. A., Crowley, J. N., Hampson, R. F., Hynes, R. G., Jenkin, M.
500 E., Rossi, M. J., and Troe, J.: Evaluated kinetic and photochemical data for atmospheric
501 chemistry: Volume II - gas phase reactions of organic species, *Atmospheric Chemistry and
502 Physics*, 6, 3625-4055, 2006.
- 503 Bannan, T. J., Booth, A. M., Bacak, A., Muller, J. B. A., Leather, K. E., Le Breton, M., Jones, B.,
504 Young, D., Coe, H., Allan, J., Visser, S., Slowik, J. G., Furger, M., Prevot, A. S. H., Lee, J.,
505 Dunmore, R. E., Hopkins, J. R., Hamilton, J. F., Lewis, A. C., Whalley, L. K., Sharp, T., Stone,
506 D., Heard, D. E., Fleming, Z. L., Leigh, R., Shallcross, D. E., and Percival, C. J.: The first UK
507 measurements of nitryl chloride using a chemical ionization mass spectrometer in central
508 London in the summer of 2012, and an investigation of the role of Cl atom oxidation, *Journal
509 of Geophysical Research-Atmospheres*, 120, 5638-5657, 2015.
- 510 Bannan, T. J., Khan, M. A. H., Le Breton, M., Priestley, M., Worrall, S. D., Bacak, A., Marsden,
511 N. A., Lowe, D., Pitt, J., Shallcross, D. E., and Percival, C. J.: A Large Source of Atomic
512 Chlorine From ClNO₂ Photolysis at a UK Landfill Site, *Geophysical Research Letters*, 46,
513 8508-8516, 2019.
- 514 Bertram, T. H., and Thornton, J. A.: Toward a general parameterization of N₂O₅ reactivity on
515 aqueous particles: the competing effects of particle liquid water, nitrate and chloride,
516 *Atmospheric Chemistry And Physics*, 9, 8351-8363, 2009.
- 517 Blank, R. R., Young, J. A., and Allen, F. L.: Aeolian dust in a saline playa environment, Nevada,
518 USA, *Journal of Arid Environments*, 41, 365-381, 1999.
- 519 Bucher, E. H., and Stein, A. F.: Large Salt Dust Storms Follow a 30-Year Rainfall Cycle in the
520 Mar Chiquita Lake (Cordoba, Argentina), *Plos One*, 11, 2016.
- 521 Crowley, J. N., Ammann, M., Cox, R. A., Hynes, R. G., Jenkin, M. E., Mellouki, A., Rossi, M. J.,
522 Troe, J., and Wallington, T. J.: Evaluated kinetic and photochemical data for atmospheric
523 chemistry: Volume V – heterogeneous reactions on solid substrates, *Atmos. Chem. Phys.*, 10,
524 9059-9223, 2010.
- 525 Eger, P. G., Friedrich, N., Schuladen, J., Shenolikar, J., Fischer, H., Tadic, I., Harder, H., Martinez,
526 M., Rohloff, R., Tauer, S., Drewnick, F., Fachinger, F., Brooks, J., Darbyshire, E., Sciare, J.,
527 Pikridas, M., Lelieveld, J., and Crowley, J. N.: Shipborne measurements of ClNO₂ in the
528 Mediterranean Sea and around the Arabian Peninsula during summer, *Atmospheric Chemistry
529 and Physics*, 19, 12121-12140, 2019.
- 530 Faxon, C. B., Bean, J. K., and Hildebrandt Ruiz, L.: Inland Concentrations of Cl₂ and ClNO₂ in
531 Southeast Texas Suggest Chlorine Chemistry Significantly Contributes to Atmospheric
532 Reactivity, *Atmosphere*, 6, 1487-1506, 2015.



- 533 Fountoukis, C., and Nenes, A.: ISORROPIA II: a computationally efficient thermodynamic
534 equilibrium model for $K^+-Ca^{2+}-Mg^{2+}-NH_4^+-Na^+-SO_4^{2-}-NO_3^- -Cl^- -H_2O$ aerosols,
535 *Atmospheric Chemistry and Physics*, 7, 4639-4659, 2007.
- 536 Frie, A. L., Dingle, J. H., Ying, S. C., and Bahreini, R.: The Effect of a Receding Saline Lake (The
537 Salton Sea) on Airborne Particulate Matter Composition, *Environmental Science & Technology*,
538 51, 8283-8292, 2017.
- 539 Fu, X., Wang, T., Wang, S., Zhang, L., Cai, S., Xing, J., and Hao, J.: Anthropogenic Emissions of
540 Hydrogen Chloride and Fine Particulate Chloride in China, *Environ Sci Technol*, 52, 1644-1654,
541 2018.
- 542 Gaston, C. J., Pratt, K. A., Suski, K. J., May, N. W., Gill, T. E., and Prather, K. A.: Laboratory
543 Studies of the Cloud Droplet Activation Properties and Corresponding Chemistry of Saline
544 Playa Dust, *Environmental Science & Technology*, 51, 1348-1356, 2017.
- 545 Gaston, C. J.: Re-examining Dust Chemical Aging and Its Impacts on Earth's Climate, *Accounts*
546 *of Chemical Research*, 53, 1005-1013, 2020.
- 547 Gholampour, A., Nabizadeh, R., Hassanvand, M. S., Taghipour, H., Nazmara, S., and Mahvi, A.
548 H.: Characterization of saline dust emission resulted from Urmia Lake drying, *Journal of*
549 *Environmental Health Science and Engineering*, 13, 2015.
- 550 Gillette, D., Stensland, G., Williams, A., Barnard, W., Gatz, D., Sinclair, P., and Johnson, T.:
551 Emissions of alkaline elements calcium, magnesium, potassium, and sodium from open sources
552 in the contiguous United States, *Global Biogeochemical Cycles*, 6, 437-457, 1992.
- 553 Gu, W., Li, Y., Zhu, J., Jia, X., Lin, Q., Zhang, G., Ding, X., Song, W., Bi, X., Wang, X., and
554 Tang, M.: Investigation of water adsorption and hygroscopicity of atmospherically relevant
555 particles using a commercial vapor sorption analyzer, *Atmospheric Measurement Techniques*,
556 10, 3821-3832, 2017.
- 557 Guo, L., Gu, W., Peng, C., Wang, W., Li, Y. J., Zong, T., Tang, Y., Wu, Z., Lin, Q., Ge, M., Zhang,
558 G., Hu, M., Bi, X., Wang, X., and Tang, M.: A comprehensive study of hygroscopic properties
559 of calcium- and magnesium-containing salts: implication for hygroscopicity of mineral dust and
560 sea salt aerosols, *Atmospheric Chemistry and Physics*, 19, 2115-2133, 2019.
- 561 Jordan, C. E., Pszenny, A. A. P., Keene, W. C., Cooper, O. R., Deegan, B., Maben, J., Routhier,
562 M., Sander, R., and Young, A. H.: Origins of aerosol chlorine during winter over north central
563 Colorado, USA, *Journal of Geophysical Research-Atmospheres*, 120, 678-694, 2015.
- 564 Kercher, J. P., Riedel, T. P., and Thornton, J. A.: Chlorine activation by N_2O_5 : simultaneous, in
565 situ detection of $ClNO_2$ and N_2O_5 by chemical ionization mass spectrometry, *Atmospheric*
566 *Measurement Techniques*, 2, 193-204, 2009.
- 567 Le Breton, M., Hallquist, A. M., Pathak, R. K., Simpson, D., Wang, Y., Johansson, J., Zheng, J.,
568 Yang, Y., Shang, D., Wang, H., Liu, Q., Chan, C., Wang, T., Bannan, T. J., Priestley, M.,
569 Percival, C. J., Shallcross, D. E., Lu, K., Guo, S., Hu, M., and Hallquist, M.: Chlorine oxidation
570 of VOCs at a semi-rural site in Beijing: significant chlorine liberation from $ClNO_2$ and
571 subsequent gas- and particle-phase Cl -VOC production, *Atmospheric Chemistry and Physics*,
572 18, 13013-13030, 2018.
- 573 Li, R., Jia, X., Wang, F., Ren, Y., Wang, X., Zhang, H., Li, G., Wang, X., and Tang, M.:
574 Heterogeneous reaction of NO_2 with hematite, goethite and magnetite: Implications for nitrate
575 formation and iron solubility enhancement, *Chemosphere*, 242, 125273-125273, 2020.
- 576 Lu, K., Guo, S., Tan, Z., Wang, H., Shang, D., Liu, Y., Li, X., Wu, Z., Hu, M., and Zhang, Y.:
577 Exploring atmospheric free-radical chemistry in China: the self-cleansing capacity and the
578 formation of secondary air pollution, *National Science Review*, 6, 579-594, 2019.



- 579 McDuffie, E. E., Fibiger, D. L., Dube, W. P., Hilfiker, F. L., Lee, B. H., Jaegle, L., Guo, H., Weber,
580 R. J., Reeves, J. M., Weinheimer, A. J., Schroder, J. C., Campuzano-Jost, P., Jimenez, J. L.,
581 Dibb, J. E., Veres, P., Ebben, C., Sparks, T. L., Wooldridge, P. J., Cohen, R. C., Campos, T.,
582 Hall, S. R., Ullmann, K., Roberts, J. M., Thornton, J. A., and Brown, S. S.: ClNO₂ Yields From
583 Aircraft Measurements During the 2015 WINTER Campaign and Critical Evaluation of the
584 Current Parameterization, *Journal of Geophysical Research-Atmospheres*, 123, 12994-13015,
585 2018a.
- 586 McDuffie, E. E., Fibiger, D. L., Dube, W. P., Lopez-Hilfiker, F., Lee, B. H., Thornton, J. A., Shah,
587 V., Jaegle, L., Guo, H., Weber, R. J., Reeves, J. M., Weinheimer, A. J., Schroder, J. C.,
588 Campuzano-Jost, P., Jimenez, J. L., Dibb, J. E., Veres, P., Ebben, C., Sparks, T. L., Wooldridge,
589 P. J., Cohen, R. C., Hornbrook, R. S., Apel, E. C., Campos, T., Hall, S. R., Ullmann, K., and
590 Brown, S. S.: Heterogeneous N₂O₅ Uptake During Winter: Aircraft Measurements During the
591 2015 WINTER Campaign and Critical Evaluation of Current Parameterizations, *Journal of*
592 *Geophysical Research-Atmospheres*, 123, 4345-4372, 2018b.
- 593 McNamara, S. M., Kolesar, K. R., Wang, S., Kirpes, R. M., May, N. W., Gunch, M. J., Cook, R.
594 D., Fuentes, J. D., Hornbrook, R. S., Apel, E. C., China, S., Laskin, A., and Pratt, K. A.:
595 Observation of Road Salt Aerosol Driving Inland Wintertime Atmospheric Chlorine Chemistry,
596 *Acs Central Science*, 6, 684-694, 2020.
- 597 Mielke, L. H., Furgeson, A., and Osthoff, H. D.: Observation of ClNO₂ in a Mid-Continental
598 Urban Environment, *Environmental Science & Technology*, 45, 8889-8896, 2011.
- 599 Mielke, L. H., Furgeson, A., Odame-Ankrah, C. A., and Osthoff, H. D.: Ubiquity of ClNO₂ in the
600 urban boundary layer of Calgary, Alberta, Canada, *Canadian Journal of Chemistry*, 94, 414-423,
601 2016.
- 602 Mitroo, D., Gill, T. E., Haas, S., Pratt, K. A., and Gaston, C. J.: ClNO₂ Production from N₂O₅
603 Uptake on Saline Playa Dusts: New Insights into Potential Inland Sources of ClNO₂, *Environ*
604 *Sci Technol*, 53, 7442-7452, 2019.
- 605 Osthoff, H. D., Roberts, J. M., Ravishankara, A. R., Williams, E. J., Lerner, B. M., Sommariva,
606 R., Bates, T. S., Coffman, D., Quinn, P. K., Dibb, J. E., Stark, H., Burkholder, J. B., Talukdar,
607 R. K., Meagher, J., Fehsenfeld, F. C., and Brown, S. S.: High levels of nitryl chloride in the
608 polluted subtropical marine boundary layer, *Nature Geoscience*, 1, 324-328, 2008.
- 609 Osthoff, H. D., Odame-Ankrah, C. A., Taha, Y. M., Tokarek, T. W., Schiller, C. L., Haga, D.,
610 Jones, K., and Vingarzan, R.: Low levels of nitryl chloride at ground level: nocturnal nitrogen
611 oxides in the Lower Fraser Valley of British Columbia, *Atmospheric Chemistry and Physics*,
612 18, 6293-6315, 2018.
- 613 Phillips, G. J., Tang, M. J., Thieser, J., Brickwedde, B., Schuster, G., Bohn, B., Lelieveld, J., and
614 Crowley, J. N.: Significant concentrations of nitryl chloride observed in rural continental Europe
615 associated with the influence of sea salt chloride and anthropogenic emissions, *Geophysical*
616 *Research Letters*, 39, 2012.
- 617 Pratt, K. A., Twohy, C. H., Murphy, S. M., Moffet, R. C., Heymsfield, A. J., Gaston, C. J., DeMott,
618 P. J., Field, P. R., Henn, T. R., Rogers, D. C., Gilles, M. K., Seinfeld, J. H., and Prather, K. A.:
619 Observation of playa salts as nuclei in orographic wave clouds, *Journal of Geophysical*
620 *Research-Atmospheres*, 115, 2010.
- 621 Ridley, D. A., Heald, C. L., Pierce, J. R., and Evans, M. J.: Toward resolution-independent dust
622 emissions in global models: Impacts on the seasonal and spatial distribution of dust,
623 *Geophysical Research Letters*, 40, 2873-2877, 2013.



- 624 Riedel, T. P., Bertram, T. H., Crisp, T. A., Williams, E. J., Lerner, B. M., Vlasenko, A., Li, S.-M.,
625 Gilman, J., de Gouw, J., Bon, D. M., Wagner, N. L., Brown, S. S., and Thornton, J. A.: Nitryl
626 Chloride and Molecular Chlorine in the Coastal Marine Boundary Layer, *Environmental*
627 *Science & Technology*, 46, 10463-10470, 2012.
- 628 Riedel, T. P., Wagner, N. L., Dube, W. P., Middlebrook, A. M., Young, C. J., Ozturk, F., Bahreini,
629 R., VandenBoer, T. C., Wolfe, D. E., Williams, E. J., Roberts, J. M., Brown, S. S., and Thornton,
630 J. A.: Chlorine activation within urban or power plant plumes: Vertically resolved ClNO₂ and
631 Cl₂ measurements from a tall tower in a polluted continental setting, *Journal of Geophysical*
632 *Research-Atmospheres*, 118, 8702-8715, 2013.
- 633 Riedel, T. P., Wolfe, G. M., Danas, K. T., Gilman, J. B., Kuster, W. C., Bon, D. M., Vlasenko, A.,
634 Li, S. M., Williams, E. J., Lerner, B. M., Veres, P. R., Roberts, J. M., Holloway, J. S., Lefer, B.,
635 Brown, S. S., and Thornton, J. A.: An MCM modeling study of nitryl chloride (ClNO₂) impacts
636 on oxidation, ozone production and nitrogen oxide partitioning in polluted continental outflow,
637 *Atmospheric Chemistry and Physics*, 14, 3789-3800, 2014.
- 638 Royer, H. M., Mitroo, D., Hayes, S. M., Haas, S. M., Pratt, K. A., Blackwelder, P. L., Gill, T. E.,
639 and Gaston, C. J.: The Role of Hydrates, Competing Chemical Constituents, and Surface
640 Composition on ClNO₂ Formation, *Environ Sci Technol*, 2021.
- 641 Ryder, O. S., Ault, A. P., Cahill, J. F., Guasco, T. L., Riedel, T. P., Cuadra-Rodriguez, L. A.,
642 Gaston, C. J., Fitzgerald, E., Lee, C., Prather, K. A., and Bertram, T. H.: On the Role of Particle
643 Inorganic Mixing State in the Reactive Uptake of N₂O₅ to Ambient Aerosol Particles,
644 *Environmental Science & Technology*, 48, 1618-1627, 2014.
- 645 Saiz-Lopez, A., and von Glasow, R.: Reactive halogen chemistry in the troposphere, *Chemical*
646 *Society Reviews*, 41, 6448-6472, 2012.
- 647 Sarwar, G., Simon, H., Xing, J., and Mathur, R.: Importance of tropospheric ClNO₂ chemistry
648 across the Northern Hemisphere, *Geophysical Research Letters*, 41, 4050-4058, 2014.
- 649 Simon, H., Kimura, Y., McGaughey, G., Allen, D. T., Brown, S. S., Osthoff, H. D., Roberts, J. M.,
650 Byun, D., and Lee, D.: Modeling the impact of ClNO₂ on ozone formation in the Houston area,
651 *Journal of Geophysical Research-Atmospheres*, 114, 2009.
- 652 Simpson, W. R., Brown, S. S., Saiz-Lopez, A., Thornton, J. A., and von Glasow, R.: Tropospheric
653 Halogen Chemistry: Sources, Cycling, and Impacts, *Chemical Reviews*, 115, 4035-4062, 2015.
- 654 Tang, M., Huang, X., Lu, K., Ge, M., Li, Y., Cheng, P., Zhu, T., Ding, A., Zhang, Y., Gligorovski,
655 S., Song, W., Ding, X., Bi, X., and Wang, X.: Heterogeneous reactions of mineral dust aerosol:
656 implications for tropospheric oxidation capacity, *Atmospheric Chemistry and Physics*, 17,
657 11727-11777, 2017.
- 658 Tang, M., Zhang, H., Gu, W., Gao, J., Jian, X., Shi, G., Zhu, B., Xie, L., Guo, L., and Gao, X.:
659 Hygroscopic properties of saline mineral dust from different regions in China: geographical
660 variations, compositional dependence and atmospheric implications, *Journal of Geophysical*
661 *Research: Atmospheres*, 124, 10844-10857, 2019.
- 662 Tang, M. J., Thieser, J., Schuster, G., and Crowley, J. N.: Kinetics and mechanism of the
663 heterogeneous reaction of N₂O₅ with mineral dust particles, *Physical Chemistry Chemical*
664 *Physics*, 14, 8551-8561, 2012.
- 665 Thaler, R. D., Mielke, L. H., and Osthoff, H. D.: Quantification of Nitryl Chloride at Part Per
666 Trillion Mixing Ratios by Thermal Dissociation Cavity Ring-Down Spectroscopy, *Analytical*
667 *Chemistry*, 83, 2761-2766, 2011.



- 668 Tham, Y. J., Yan, C., Xue, L., Zha, Q., Wang, X., and Wang, T.: Presence of high nitryl chloride
669 in Asian coastal environment and its impact on atmospheric photochemistry, *Chinese Science*
670 *Bulletin*, 59, 356-359, 2014.
- 671 Tham, Y. J., Wang, Z., Li, Q., Yun, H., Wang, W., Wang, X., Xue, L., Lu, K., Ma, N., Bohn, B.,
672 Li, X., Kecorius, S., Groess, J., Shao, M., Wiedensohler, A., Zhang, Y., and Wang, T.:
673 Significant concentrations of nitryl chloride sustained in the morning: investigations of the
674 causes and impacts on ozone production in a polluted region of northern China, *Atmospheric*
675 *Chemistry and Physics*, 16, 14959-14977, 2016.
- 676 Tham, Y. J., Wang, Z., Li, Q., Wang, W., Wang, X., Lu, K., Ma, N., Yan, C., Kecorius, S.,
677 Wiedensohler, A., Zhang, Y., and Wang, T.: Heterogeneous N₂O₅ uptake coefficient and
678 production yield of ClNO₂ in polluted northern China: roles of aerosol water content and
679 chemical composition, *Atmospheric Chemistry and Physics*, 18, 13155-13171, 2018.
- 680 Thornton, J. A., Kercher, J. P., Riedel, T. P., Wagner, N. L., Cozic, J., Holloway, J. S., Dube, W.
681 P., Wolfe, G. M., Quinn, P. K., Middlebrook, A. M., Alexander, B., and Brown, S. S.: A large
682 atomic chlorine source inferred from mid-continental reactive nitrogen chemistry, *Nature*, 464,
683 271-274, 2010.
- 684 Wang, H., Chen, J., and Lu, K.: Development of a portable cavity-enhanced absorption
685 spectrometer for the measurement of ambient NO₃ and N₂O₅: experimental setup, lab
686 characterizations, and field applications in a polluted urban environment, *Atmospheric*
687 *Measurement Techniques*, 10, 1465, 2017a.
- 688 Wang, H., Lu, K., Guo, S., Wu, Z., Shang, D., Tan, Z., Wang, Y., Le Breton, M., Lou, S., Tang,
689 M., Wu, Y., Zhu, W., Zheng, J., Zeng, L., Hallquist, M., Hu, M., and Zhang, Y.: Efficient N₂O₅
690 uptake and NO₃ oxidation in the outflow of urban Beijing, *Atmospheric Chemistry and Physics*,
691 18, 9705-9721, 2018.
- 692 Wang, H., Tang, M., Tan, Z., Peng, C., and Lu, K.: Atmospheric Chemistry of Nitryl Chloride,
693 *Progress in Chemistry*, 32, 1535-1546, 2020a.
- 694 Wang, T., Tham, Y. J., Xue, L., Li, Q., Zha, Q., Wang, Z., Poon, S. C. N., Dube, W. P., Blake, D.
695 R., Louie, P. K. K., Luk, C. W. Y., Tsui, W., and Brown, S. S.: Observations of nitryl chloride
696 and modeling its source and effect on ozone in the planetary boundary layer of southern China,
697 *Journal of Geophysical Research-Atmospheres*, 121, 2476-2489, 2016.
- 698 Wang, X., Hua, T., Zhang, C., Lang, L., and Wang, H.: Aeolian salts in Gobi deserts of the western
699 region of Inner Mongolia: Gone with the dust aerosols, *Atmospheric Research*, 118, 1-9, 2012.
- 700 Wang, X., Wang, H., Xue, L., Wang, T., Wang, L., Gu, R., Wang, W., Tham, Y. J., Wang, Z.,
701 Yang, L., Chen, J., and Wang, W.: Observations of N₂O₅ and ClNO₂ at a polluted urban surface
702 site in North China: High N₂O₅ uptake coefficients and low ClNO₂ product yields,
703 *Atmospheric Environment*, 156, 125-134, 2017b.
- 704 Wang, X., Jacob, D. J., Eastham, S. D., Sulprizio, M. P., Zhu, L., Chen, Q., Alexander, B., Sherwen,
705 T., Evans, M. J., Lee, B. H., Haskins, J. D., Lopez-Hilfiker, F. D., Thornton, J. A., Huey, G. L.,
706 and Liao, H.: The role of chlorine in global tropospheric chemistry, *Atmospheric Chemistry and*
707 *Physics*, 19, 3981-4003, 2019.
- 708 Wang, X., Jacob, D. J., Fu, X., Wang, T., Le Breton, M., Hallquist, M., Liu, Z., McDuffie, E. E.,
709 and Liao, H.: Effects of Anthropogenic Chlorine on PM_{2.5} and Ozone Air Quality in China,
710 *Environmental Science & Technology*, 54, 9908-9916, 2020b.
- 711 Wang, X., Jacob, D. J., Downs, W., Zhai, S., Zhu, L., Shah, V., Holmes, C. D., Sherwen, T.,
712 Alexander, B., Evans, M. J., Eastham, S. D., Neuman, J. A., Veres, P., Koenig, T. K., Volkamer,
713 R., Huey, L. G., Bannan, T. J., Percival, C. J., Lee, B. H., and Thornton, J. A.: Global



- 714 tropospheric halogen (Cl, Br, I) chemistry and its impact on oxidants, *Atmos. Chem. Phys.*
715 *Discuss.*, 2021, 1-34, 2021.
- 716 Wang, Z., Wang, W. H., Tham, Y. J., Li, Q. Y., Wang, H., Wen, L., Wang, X. F., and Wang, T.:
717 Fast heterogeneous N₂O₅ uptake and ClNO₂ production in power plant and industrial plumes
718 observed in the nocturnal residual layer over the North China Plain, *Atmospheric Chemistry*
719 *and Physics*, 17, 12361-12378, 2017c.
- 720 Wu, C., Zhang, S., Wang, G., Lv, S., Li, D., Liu, L., Li, J., Liu, S., Du, W., Meng, J., Qiao, L.,
721 Zhou, M., Huang, C., and Wang, H.: Efficient Heterogeneous Formation of Ammonium Nitrate
722 on the Saline Mineral Particle Surface in the Atmosphere of East Asia during Dust Storm
723 Periods, *Environmental science & technology*, 54, 15622-15630, 2020.
- 724 Young, C. J., Washenfelder, R. A., Edwards, P. M., Parrish, D. D., Gilman, J. B., Kuster, W. C.,
725 Mielke, L. H., Osthoff, H. D., Tsai, C., Pikelnaya, O., Stutz, J., Veres, P. R., Roberts, J. M.,
726 Griffith, S., Dusanter, S., Stevens, P. S., Flynn, J., Grossberg, N., Lefer, B., Holloway, J. S.,
727 Peischl, J., Ryerson, T. B., Atlas, E. L., Blake, D. R., and Brown, S. S.: Chlorine as a primary
728 radical: evaluation of methods to understand its role in initiation of oxidative cycles,
729 *Atmospheric Chemistry and Physics*, 14, 3427-3440, 2014.
- 730 Yu, C., Wang, Z., Xia, M., Fu, X., Wang, W., Tham, Y. J., Chen, T., Zheng, P., Li, H., Shan, Y.,
731 Wang, X., Xue, L., Zhou, Y., Yue, D., Ou, Y., Gao, J., Lu, K., Brown, S. S., Zhang, Y., and
732 Wang, T.: Heterogeneous N₂O₅ reactions on atmospheric aerosols at four Chinese sites:
733 improving model representation of uptake parameters, *Atmos. Chem. Phys.*, 20, 4367-4378,
734 2020.
- 735 Zhang, H., Gu, W., Li, Y. J., and Tang, M.: Hygroscopic properties of sodium and potassium salts
736 as related to saline mineral dusts and sea salt aerosols, *Journal of environmental sciences*, 95,
737 65-72, 2020.
- 738 Zhang, X., Zhuang, G., Yuan, H., Rahn, K. A., Wang, Z., and An, Z.: Aerosol Particles from Dried
739 Salt-Lakes and Saline Soils Carried on Dust Storms over Beijing, *Terrestrial Atmospheric and*
740 *Oceanic Sciences*, 20, 619-628, 2009.
- 741 Zhang, X. X., Sharratt, B., Liu, L. Y., Wang, Z. F., Pan, X. L., Lei, J. Q., Wu, S. X., Huang, S. Y.,
742 Guo, Y. H., Li, J., Tang, X., Yang, T., Tian, Y., Chen, X. S., Hao, J. Q., Zheng, H. T., Yang, Y.
743 Y., and Lyu, Y. L.: East Asian dust storm in May 2017: observations, modelling, and its
744 influence on the Asia-Pacific region, *Atmos. Chem. Phys.*, 18, 8353-8371, 2018.
- 745 Zheng, B., Tong, D., Li, M., Liu, F., Hong, C., Geng, G., Li, H., Li, X., Peng, L., Qi, J., Yan, L.,
746 Zhang, Y., Zhao, H., Zheng, Y., He, K., and Zhang, Q.: Trends in China's anthropogenic
747 emissions since 2010 as the consequence of clean air actions, *Atmospheric Chemistry and*
748 *Physics*, 18, 14095-14111, 2018.
- 749